ADVANCES IN ATMOSPHERIC SCIENCES, VOL. 37, MAY 2020, 441–454

• **Original Paper** •

Impact of Assimilation of Radiosonde and UAV Observations from the Southern Ocean in the Polar WRF Model

Qizhen SUN*[1,2], Timo VIHMA[3], Marius O. JONASSEN[4,5], and Zhanhai ZHANG[1,6]

[1]*College of Oceanic and Atmospheric Sciences*, *Ocean University of China*, *Qingdao* 266100, *China*

[2]*Polar Research and Forecasting Division*, *National Marine Environmental Forecasting Center*, *Beijing* 100081, *China*

[3]*Finnish Meteorological Institute*, *PO Box* 503, *Helsinki FI* 00101, *Finland*

[4]*Geophysical Institute*, *University of Bergen*, *PO Box* 7803, *Bergen NO* 5020, *Norway*

[5]*The University Centre in Svalbard*, *PO Box* 156, *Longyearbyen NO* 9171, *Norway*

[6]*Key Laboratory for Polar Science of the State Oceanic Administration*, *Polar Research Institute of China*, *Shanghai* 200136, *China*

(Received 6 October 2019; revised 23 January 2020; accepted 8 February 2020)

ABSTRACT

Weather forecasting in the Southern Ocean and Antarctica is a challenge above all due to the rarity of observations to be assimilated in numerical weather prediction (NWP) models. As observations are expensive and logistically challenging, it is important to evaluate the benefit that additional observations could bring to NWP. Atmospheric soundings applying unmanned aerial vehicles (UAVs) have a large potential to supplement conventional radiosonde sounding observations. Here, we applied UAV and radiosonde sounding observations from an RV Polarstern cruise in the ice-covered Weddell Sea in austral winter 2013 to evaluate the impact of their assimilation in the Polar version of the Weather Research and Forecasting (Polar WRF) model. Our experiments revealed small to moderate impacts of radiosonde and UAV data assimilation. In any case, the assimilation of sounding data from both radiosondes and UAVs improved the analyses of air temperature, wind speed, and humidity at the observation site for most of the time. Further, the impact on the results of 5-day-long Polar WRF experiments was often felt over distances of at least 300 km from the observation site. All experiments succeeded in capturing the main features of the evolution of near-surface variables, but the effects of data assimilation varied between different cases. Due to the limited vertical extent of the UAV observations, the impact of their assimilation was limited to the lowermost 1–2-km layer, and assimilation of radiosonde data was more beneficial for modeled sea level pressure and near-surface wind speed.

Key words: numerical weather prediction, radiosonde soundings, unmanned aerial vehicles, data assimilation, Antarctic, Southern Ocean

Citation: Sun, Q. Z., T. Vihma, M. O. Jonassen, and Z. H. Zhang, 2020: Impact of assimilation of radiosonde and UAV observations from the Southern Ocean in the Polar WRF model. *Adv. Atmos. Sci.*, **37**(5), 441–454, https://doi.org/10.1007/s00376-020-9213-8.

Article Highlights:

- Assimilation of radiosonde and UAV data improved the forecasts of air temperature, wind speed, and air humidity at the observation site.
- Assimilation of radiosonde data was more beneficial than that of UAV data, due to the higher vertical extent of the radiosonde data.
- UAVs may be widely used in the future for sounding throughout the troposphere owing to their advantages in the Antarctic.

1. Introduction

Observations from the Southern Ocean and Antarctica are pivotal for climate research (e.g., Rintoul et al., 2012; Jones et al., 2016) and operational weather forecasting (Turner and Pendlebury, 2004). However, the amount of in-situ observations from these regions is very limited. From the point of view of numerical weather prediction (NWP), there is a particular need for more in-situ observations on

* Corresponding author: Qizhen SUN
Email: sunqizhen@nmefc.cn

the profiles of atmospheric pressure, temperature, moisture and wind. These are important for initialization of NWP models (Bromwich et al., 2005), for which near-surface observations from weather stations and buoys alone are not sufficient. In addition, observations on profiles are needed for the evaluation of NWP model results (Atlaskin and Vihma, 2012; Wille et al., 2017).

Large amounts of profile observations are collected via satellite remote sensing, and such data are routinely assimilated into NWP models. Microwave radiances sensitive to temperature and humidity have been a vital part of global observing systems since the 1990s (Derber and Wu, 1998). With a parameterization of surface snow and sea ice emissivity, assimilation of these radiances has yielded important information on the profiles of air temperature and humidity profiles (Karbou, 2014). This is the case particularly in regions where very few in-situ observations are assimilated. For example, Bouchard et al. (2010) found that the assimilation of microwave and infrared data over Antarctica impacts spatial patterns of variables, such as snowfall. Singh et al. (2012) showed that assimilation of radiances and retrieval measurements with the Atmospheric Infrared Sounder has a significant impact on analysis and short-range forecasts. The improvement was mostly found in forecasts for moisture, temperature, wind and rainfall. However, compared to radiosonde soundings, satellite remote sensing data on atmospheric profiles are not equally accurate and have a much worse vertical resolution (Boylan et al., 2015). For example, Naakka et al. (2019) showed that satellite observations cannot compensate for the large spatial gap in the radiosonde sounding network in the Arctic. In Antarctica and the Southern Ocean, the spatial gaps are even much larger, as the radiosonde sounding stations are mostly located along the coastline (e.g., Turner and Pendlebury, 2004). This suggest that there is a need for more radiosonde soundings or other in-situ observations of profiles of temperature, humidity and wind over the Southern Ocean and the inner parts of the Antarctic ice sheet.

The impact of assimilation of radiosonde data from polar Regions to NWP models has so far been studied mostly in the Arctic. Sato et al. (2017) showed that campaign-based radiosonde observations from the Arctic, assimilated in an NWP model, reduced analysis errors in the upper troposphere, and thus improved forecast skill and reduced uncertainties of predicted weather extremes in remote locations. In Yamazaki et al. (2015) even a few radiosonde observations had considerable influence on the forecasting of an Arctic cyclone. Inoue et al. (2013) investigated the impact of radiosonde data from the ice-free Arctic Ocean with a focus on the density of the observing network. They found that frequent radiosonde observations over the Arctic Ocean improved the accuracy of an experimental ensemble reanalysis both locally and throughout the northern half of the Northern Hemisphere, with the impact lasting even for weeks. However, according to Agustí-Panareda et al. (2010), the impacts of radiosonde data on short-range forecasts may disappear after 24 h. The abovementioned results suggest that the impacts of radiosonde assimilation depend on the case studied and potentially on the experimental setup.

In addition to improving weather forecasting, assimilation of sounding data is also useful to improve sea-ice predictions. Using a coupled ice–ocean model, Inoue et al. (2015) found that assimilation of campaign-based radiosonde data from the Arctic helped to predict a strong wind event, and consequently the wind-driven sea-ice advection. Further, Ono et al. (2016) showed that assimilation of radiosonde data yielded better predictions for the sea-ice distribution, in particular in a case with a strong cyclone near the sounding site.

In-situ observations of upper-air temperature, wind, and specific humidity are also available from aircraft and, for wind, pilot balloons and wind profilers (e.g. Dee et al., 2011; Murphy et al., 2014; Driemel et al., 2016). These observations could also play a critical role in modern NWP systems, especially at high latitudes where in-situ observations are rare (e.g., Bumbaco et al., 2014). However, benefits from assimilation of radiosonde and wind profiler data have been detected also for short-range forecasts for Central Europe (Federico, 2013), and studies on temperature and humidity retrievals from satellite and ground-based microwave radiometers and their assimilation into NWP system have also been made (e.g., Knupp et al., 2009; Guedj et al., 2010; Caumont et al., 2016).

Due to recent technological advances, atmospheric soundings can also be made applying unmanned aerial vehicles (UAVs). As one type of UAV, the small unmanned meteorological observer (SUMO) has proven its applicability for a wide range of in-situ ABL research applications, even under polar conditions (Reuder et al., 2009; Mayer, 2011; Cassano, 2014; Båserud et al., 2016; Kral et al., 2018). Jonassen et al. (2012), Passner et al. (2012) and Ágústsson et al. (2014) have shown how temperature, humidity, and wind profiles from the lower troposphere obtained with SUMO can be used to improve numerical weather simulations applying the Weather Research and Forecasting (WRF) model. In the study of Ágústsson et al. (2014), atmospheric profiles retrieved by SUMO near a high mountain in Iceland were assimilated in the Advanced Research version of WRF. The complex weather situation was captured, when WRF was forced with the observed profiles of wind and temperature. Passner et al. (2012) showed that the impact of data assimilation did not only occur downwind but also upwind of the observation site.

Campaigns applying SUMO have also recently been carried out in coastal sites of Antarctica (Knuth et al., 2013; Cassano et al., 2016). A unique observation campaign with SUMO flight missions supplementing daily radiosonde soundings took place in the Southern Ocean from 21 June to 4 August 2013, when RV Polarstern cruised in the ice-covered Weddell Sea during its winter expedition, ANT-XXIX/6 (Jonassen et al., 2015; Fig. 1). In this study, the Polar version of WRF (Polar WRF, version 3.7.1) was employed to carry out experiments on the impact of assimila-

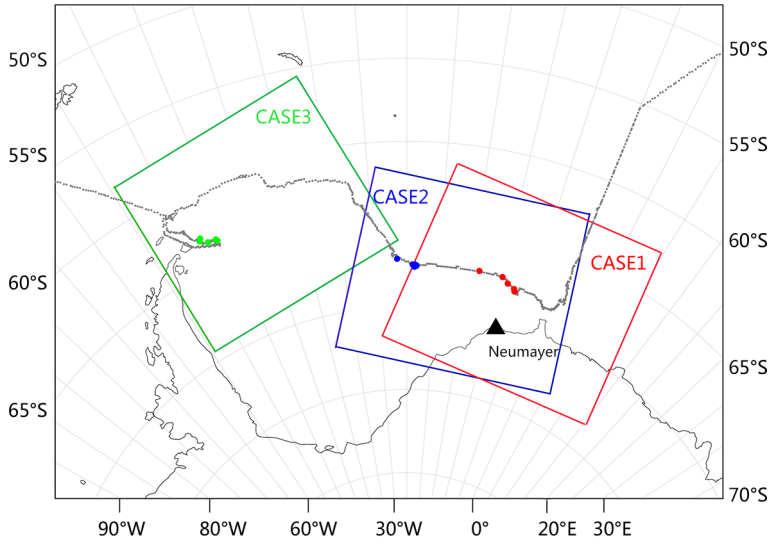

Fig. 1. Domains of Polar WRF and the track of RV Polarstern (gray dots) with the ship locations during the periods of three modeling cases marked as red dots for CASE1, blue for CASE2, and green for CASE3.

tion of RV Polarstern radiosonde and UAV observations on the model analyses and simulations. The aim of this study was to find out, for the first time, what the benefit is of radiosonde and UAV observations for an NWP model over the Southern Ocean in winter.

2. Data and strategy

2.1. *Observations*

2.1.1. *SUMO soundings*

SUMO is based on a commercially available construction kit called FunJet by Multiplex, equipped with an autopilot and meteorological sensors by Lindenberg und Müller GmbH &. Co, to measure profiles of meteorological variables (Reuder et al., 2009). During the cruise of RV Polarstern (Fig. 1), SUMO observations of the profiles of air temperature, humidity and wind were started on 21 June 2013 and ended on 4 August (Jonassen et al., 2015). In this study, we applied SUMO observations from three periods: 3 July, 11 to 14 July, and 31 July to 4 August, on which dates the wind was gentle or a moderate breeze according to the meteorological observations during POLARSTERN cruise ANT-XXIX/6 (König-Langlo, 2013a). The weather conditions at the sounding sites during the three periods are described in Table 1. The cruise with RV Polarstern was divided into different ice stations, and the three periods correspond to three of these ice stations.

Each SUMO flight lasted for approximately 30 minutes and included two profiles: the ascent and the descent. The temperature and humidity sensors have a thermal inertia, and the descent rate of SUMO is slightly slower than the ascent rate. Hence, data from the descent profile are more accurate, and we only applied these in the assimilation experiments. We are aware that there are numerical methods to correct for sensor lag (e.g., Miloshevich et al., 2004, Jonassen and Reuder, 2008). However, in the lower troposphere, particularly at altitudes below 100 m, temperature and humidity profiles often have a rather strong vertical variability. Such profiles are particularly challenging to correct for sensor lag, as outlined by Jonassen and Reuder (2008), and we chose therefore not to apply such correction to the profiles.

Prior to the experiments, the data quality was controlled as follows:

(1) The time of observation of the SUMO profiles was defined as the time corresponding to the middle of the descent. During the landing, SUMO was controlled manually, and its track is not as constant as when it is at higher levels. Thus, wind observations at altitudes below 70 m were excluded. For pressure, humidity, and temperature, the threshold altitude was 15 m.

(2) If the difference of the temperature profiles of the ascent and descent at the lowermost tens of meters exceeded 2°C, these temperature data were regarded as unreliable and were not used.

(3) Each SUMO profile was averaged over 10-m height intervals.

2.1.2. *Radiosonde soundings on Polarstern*

The radiosonde equipment aboard RV Polarstern was employed to carry out daily (1100 UTC) profile measurements of pressure, temperature, relative humidity, and the wind vector (König-Langlo, 2013b). As solar and infrared radiation may significantly affect the accuracy of radiosonde temperatures at high altitudes (Luers and Eskridge, 1998; National Weather Service, 2019), data above 12 km were excluded. Balloons aboard Polarstern were launched from the helicopter deck at 10 m above sea level (ASL). The lowest individual record of radiosonde observations at 10 m was neglected to avoid flow disturbance and heating effects of the vessel (which may be large, if the radiosonde

Table 1. SUMO and radiosonde observations assimilated in Polar WRF in this study. The weather by the time of SUMO operations is listed in the form of WMO Present weather codes. The corresponding meanings of the codes are: 01, cloud generally dissolving or becoming less developed; 03, clouds generally forming or developing; 11, patches of shallow fog or ice fog at the station; 12, more or less continuous shallow fog or ice fog at the station; 70, intermittent fall of snowflakes, slight at time of observations; 71, continuous fall of snowflakes, slight at time of observations; 76, diamond dust; 77, snow grains.

(a) CASE1

Data source	Observation date and time (UTC)	Top height (km)
Radiosonde	3 July 10:45; 4 July 10:46; 5 July 10:36; 6 July 09:01; 7 July 09:03; 8 July 09:09	24
SUMO	22 observations on 3 July, from 13:17 to 22:16; Present weather code: 76	1.1

(b) CASE2

Data source	Observation date and time (UTC)	Top height (km)
Radiosonde	11 July 10:31; 12 July 10:31; 13 July 10:32; 14 July 10:42; 15 July 10:41; 16 July 10:44	25
SUMO	24 observations on 11 July, from 14:21 to 23:59; Present weather code: 77, 71; 32 observations on 13 July, from 12:57 to 20:54; Present weather code: 70; 18 observations on 14 July, from 14:01 to 18:01; Present weather code: 12	1.1

(c) CASE3

Data source	Observation date and time (UTC)	Top height (km)
Radiosonde	31 July 11:01; 1 August 11:05; 2 August 11:02; 3 August 11:02; 4 August 11:04; 5 August 10:58	23
SUMO	20 observations on 31 July, from 12:49 to 21:33; Present weather code: 11; 6 observations on 2 August, from 12:21 to 13:41; Present weather code: 03; 10 observations on 4 August, from 19:46 to 21:57; Present weather code: 77, 01	1.6 – 1.7

launching site is located downwind of the ship superstructures). At altitudes above the highest mast (approximately 45 m), we do not expect effects of the ship on the data. Radiosonde profile data of atmospheric pressure, wind speed and direction, as well as air temperature and humidity, were used in the data assimilation experiments. The vertical resolution of the radiosonde observations was approximately 30 m, and no vertical averages were taken. For a typical radiosonde profile, there were approximately 400 levels of records. The radiosonde and SUMO observations assimilated in the Polar WRF experiments are listed in Table 1.

2.1.3. *Observations from automatic weather stations*

In addition to the profile observations from SUMO and radiosondes, observations from the automatic weather station (AWS) aboard RV Polarstern were used to verify the results of the simulations. For this study, hourly records of atmospheric pressure, air temperature, air humidity, and wind were acquired at the heights of 16, 29, 29, and 39 m ASL, respectively. The atmospheric pressure measurements were reduced to the sea level. The true winds were calculated taking into account GPS and gyro heading data on the movement of the ship. Data from windward sensors of temperature and humidity, mounted in unventilated radiation shields, were used. For the comparisons against model results, the values at model levels were interpolated to the AWS observation levels. In addition, meteorological observations from the Neumayer III station in Dronning Maud Land, Antarctica, were utilized.

2.2. *Polar WRF model*

Polar WRF is a polar-optimized NWP model, which contains important modifications for a better presentation of physical processes in polar regions (Hines and Bromwich, 2008). Polar WRF is applied in operational weather forecasting in the Antarctic mostly by the U.S. Antarctic Mesoscale Prediction System (AMPS; Bromwich et al., 2005), run for the entire continent and surrounding seas (Powers et al., 2012), but also by the Chinese National Marine Environmental Forecasting Center for Chinese stations and ships. Polar WRF was also applied in the Arctic System Reanalysis (Bromwich et al., 2016), and is widely used for Arctic and Antarctic weather and climate research. The performance of Polar WRF has been assessed in the Arctic and Antarctic (Bromwich et al., 2013; Hines et al., 2017; Wille et al., 2017).

The physical parameterizations of the Polar WRF model (version 3.7.1) used in this study followed those applied in AMPS. The Mellor–Yamada–Janjic scheme (Janjić, 2001) was applied for the atmospheric boundary layer, the Janjic-eta scheme, based on Monin–Obukhov similarity theory, for surface exchange processes, the Grell–Devenyi scheme (Grell and Dévényi, 2002) for clouds, and the Rapid Radiative Transfer Model for General Circulation Models scheme (Iacono et al., 2008) for radiation. The combination of parameterizations applied in AMPS has been tested by Bromwich et al. (2013) and shows promising skill in weather forecasting. The initial and boundary conditions were extracted from the ECMWF operational analysis at a 0.125° spatial and 6-h temporal resolution. The WRF four-dimensional data assimilation (FDDA) system was used to assimilate the radiosonde and SUMO data from RV Polarstern. Here, we applied Polar WRF in three domains (Fig. 1), each having 232 × 205 grid points with a horizontal resolution of 6 km, and 61 layers in the vertical. The three domains were designed in such way to cover the sounding sites and the downstream areas. The prognostic equations were solved with a time step of 60

seconds.

2.3. *Data assimilation strategy*

Corresponding to the particular periods of SUMO observations (3 July, 11–14 July, and 31 July to 4 August), three simulation cases were designed in this study (hereinafter referred to as CASE1, CASE2 and CASE3, respectively).

To evaluate the potential benefit from assimilation of the observed profile data from radiosonde and SUMO soundings, a set of numerical model simulations was conducted. Each case included three independent Polar WRF experiments: CTRL (the control experiment, without any observation assimilated), SUMOE (experiment with SUMO observations assimilated), and RSE (experiment with radiosonde observations of RV Polarstern assimilated). For each experiment in each case, the length of the simulation period was 5 days and 12 hours, starting from 0000 UTC on the first day of each observation period. Accordingly, for CASE1 the simulation period was from 0000 UTC 3 July to 1200 UTC 8 July; for CASE2, from 0000 UTC 11 July to 1200 UTC 16 July; for CASE3, from 0000 UTC 31 July to 1200 UTC 5 August. To allow an appropriate adjustment of the lower boundary conditions to the physics of the model, the first approximately 12 hours of each case was a spin-up period of the model integration (with ECMWF initial and boundary conditions, which was updated every 6 hours), and after that the first SUMO and/or radiosonde observations were assimilated (Table 1).

As an FDDA method, observational nudging uses observation data to push (or nudge) model values toward observations, and continuously merges observations into model simulations in order to keep model predictions from drifting away from observations. In this study, observational nudging was used to locally force the simulations towards the SUMO and radiosonde observations. Variables including pressure, height, humidity, wind and temperature were used in the assimilation experiments, and the time window for the assimilation of each profile was 2 hours. Thus, the impacts of these observations on simulations can be evaluated.

3. Impacts of data assimilation

3.1. *Impacts on local analyses*

To demonstrate how the assimilation process of sounding data affects the model analyses, Fig. 2 compares the observed profiles and the analyses of the CTRL, RSE and SUMOE experiments. These profiles were extracted from the first analyses (after assimilation of the first observations approximately 12 hours after the start of the experiment) in CASE2 and CASE3, interpolated at the position of Polarstern at the time of observations. The comparisons related to analyses of CASE1 are not presented because the time of radiosonde observations on 3 July, which was the simulation period of CASE1, were all in the morning and they did not overlap with the time of SUMO observations. The temperature, wind and relative humidity analyses including the assimilation of radiosonde observations (two leftmost columns in Fig. 2) and SUMO observations (two rightmost columns in Fig. 2) match the observed profiles better than the CTRL analyses. The positive impact of radiosonde observations, i.e., the RSE assimilated profile is closer to the observations than is the CTRL, and is large for air temperatures in the lowermost 2-km layer on 11 July, for mid- and upper-tropospheric wind speeds on 11 July, and for tropospheric relative humidity on 11 and 31 July. In the case of SUMO observations, the positive impact is large for air temperatures in the lowermost 1-km layer on 11 July, for near-surface wind speeds on 11 July, and for relative humidity in the lowermost 1–2-km layer on 11 and 31 July. In addition to the different observation heights, the differences in the impact of radiosonde and SUMO data may also be affected by the time difference between radiosonde and SUMO observations. Also, note that the wind speed profile is also affected by assimilation of data on the mean sea level pressure (MSLP) and air temperature profile.

Compared to temperature profiles, the wind and humidity profiles based on radiosonde and SUMO data assimilation do not follow the details of the observed profiles as well as they do in the case of temperature profiles, but they still capture well the main characteristics of the observations. At high altitudes, where SUMO observations are absent, the profiles of the SUMOE experiment tend to approach the profiles of the CTRL experiment. The main message of Fig. 2 is that assimilation of radiosonde and SUMO data has a clear positive effect on the local analyses.

3.2. *Impacts on the 5-day model experiments along the track of RV Polarstern*

The impacts of data assimilation on the 5-day model experiments are examined by comparing the time series of several variables along the cruise track of RV Polarstern. Observations from the AWS aboard the vessel are used as a reference. The model results from the three groups of simulations were interpolated to the ship track using the model output for the nearest four grid points at each time step. The time series of the difference between simulations and observations (simulations minus observations) of the three cases are shown in Fig. 3 for air temperature, MSLP, wind speed and direction, as well as relative and specific humidity.

For most of the time in the three cases, all the three experiments underestimate the air temperature (Fig. 3, first row). Soon after radiosonde soundings (indicated by red crosses on the horizontal axis), RSE often yields better results than CTRL and SUMOE. However, CTRL and SUMOE are almost identical, except in the first half of CASE2 when most of the SUMO observations are assimilated. In this period, there is an improvement in SUMOE against CTRL. Minor positive effects of SUMO data assimilation are also found in CASE1 and CASE3.

Results for MSLP are slightly positively impacted by assimilation of SUMO observations in the three cases compared with CTRL (Fig. 3, second row; blue dots indicate the

SUMO observation times). However, in CASE1 and CASE3 the positive impact disappears shortly after the assimilation. RSE yields unreasonable noise at the times when radiosonde observations are assimilated, especially in CASE1.

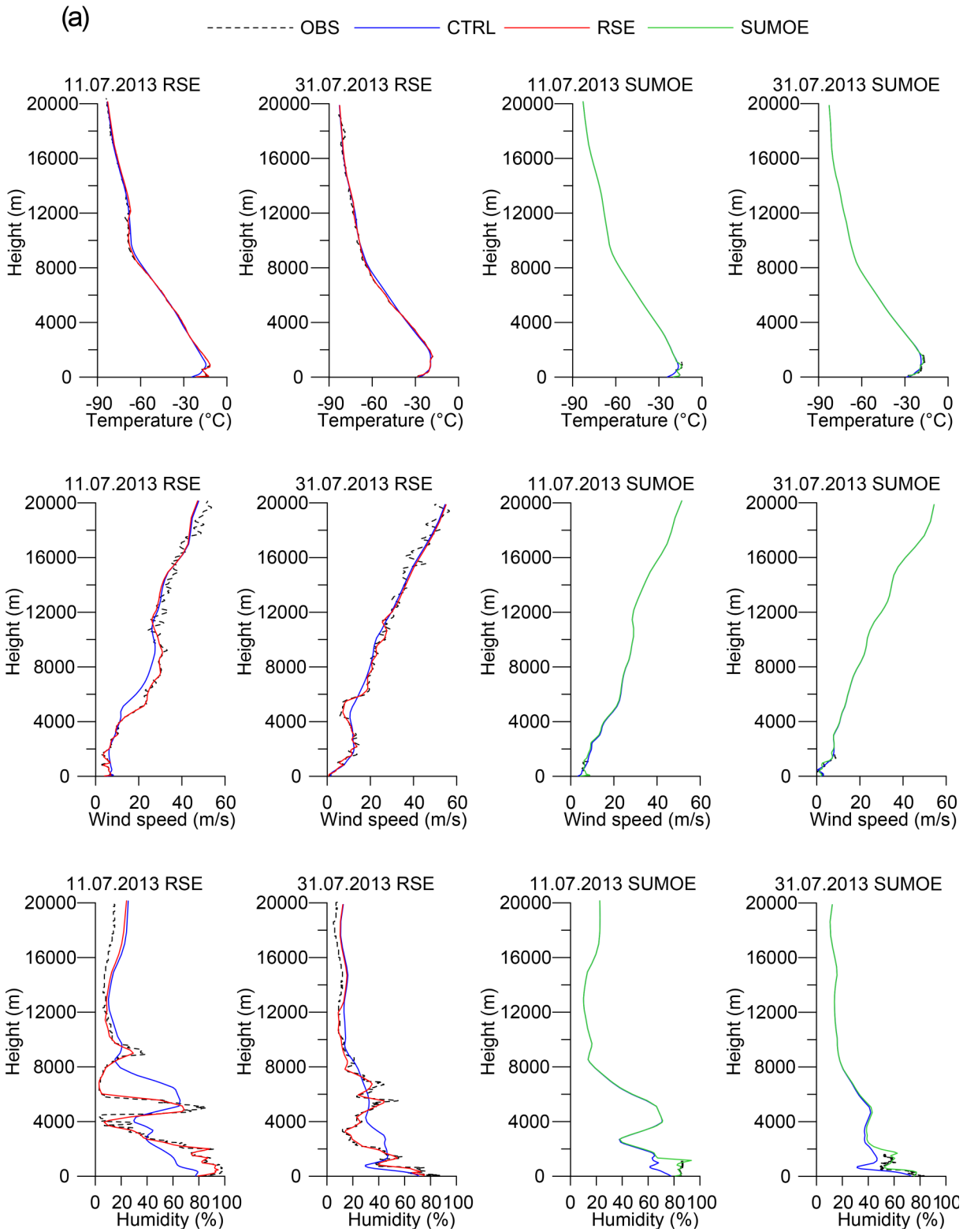

Fig. 2. (a) Profiles of air temperature, wind speed and relative humidity based on radiosonde observations (black dotted lines in two leftmost columns), SUMO observations (black dotted lines in two rightmost columns), analysis of CTRL (blue lines), analysis of RSE (red lines), and analysis of SUMOE (green lines). The analysis times of RSE and SUMOE in the four columns are 1031 UTC 11 July, 1101 UTC 31 July, 1421 UTC 11 July, and 1249 UTC 31 July, respectively. (b) The same plots for SUMOE and CTRL but zoomed in for the lowermost 2 km only.

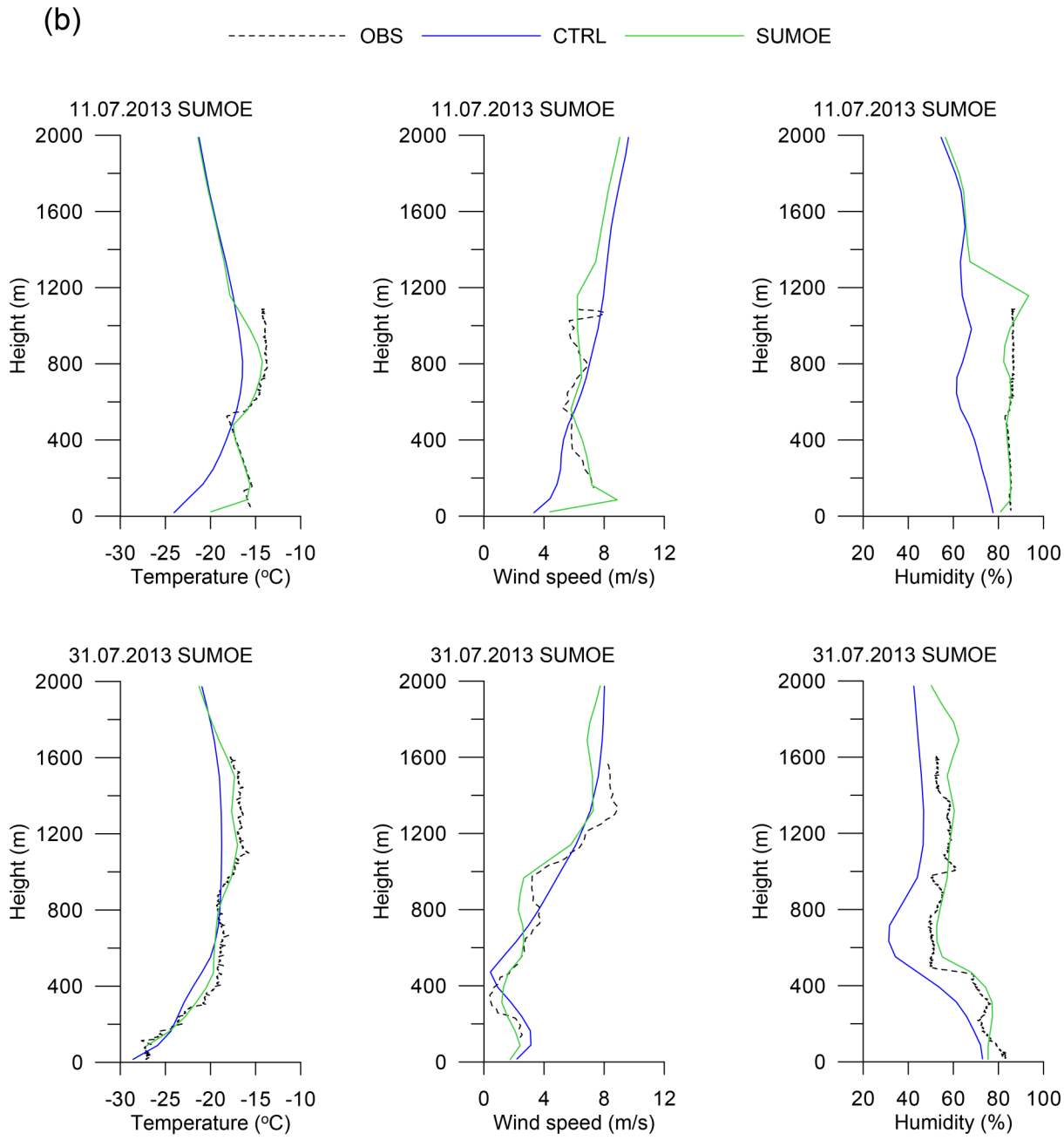

Fig. 2. (Continued).

Noise is generated also on the fifth day of CASE2 and CASE3. In the first half of CASE2, RSE also shows a positive impact on the air pressure.

The benefit from the assimilation of profile observations to simulated near-surface wind speed (Fig. 3, third and fourth rows) is not as clear as in the case of temperature and pressure. Minor improvements could still be found at the times when SUMO observations are available for assimilation. RSE shows better skill than SUMOE in the simulation of wind direction in CASE1. SUMOE and RSE are slightly better than CTRL in the simulation of relative and specific humidity, especially at times when observations are assimilated. All three simulations underestimate relative and specific humidity in all cases.

In general, all the experiments succeeded in capturing the main features of the evolution of near-surface variables. It is worth noting that the number of observations varies between and during the three cases, and this may be one of the reasons why the benefit from the assimilation of different sounding data varies from time to time and from case to case. In addition, during the three cases, the vessel traveled mainly northwestward against the westerly wind. Thus, it is understandable that the assimilated sounding data cannot have much impact when evaluated against observations taken at a vessel located upstream of the observation site.

In addition to the model results along the track of RV Polarstern, the impact of assimilation on the simulations for Antarctic stations is also of interest. Figure 4 shows the simu-

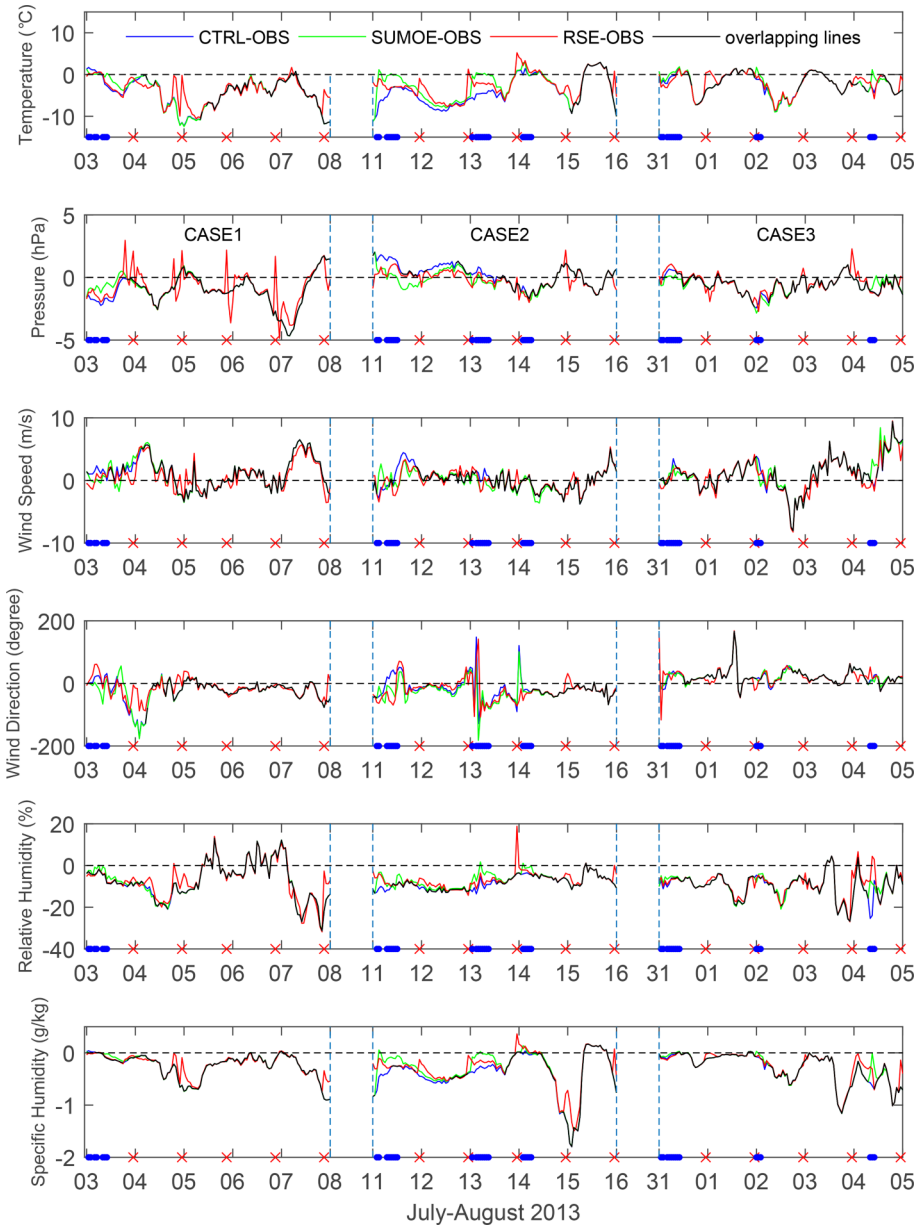

Fig. 3. Time series of the model bias for temperature (*T*), mean-sea-level pressure (*P*), wind speed (WS), wind direction (WD), relative humidity (RH), and specific humidity (SH) along the track of RV Polarstern during the three cases. For WD, a positive bias indicates clockwise turning while a negative bias indicates anticlockwise turning. The black solid lines show time periods when the difference between CTRL and SUMOE (or RSE) are less than 5% of the corresponding vertical axis scale. The numbers beneath the horizontal axis indicate the dates of July and August 2013. For each case, the time series starts at 1200 UTC on the first day of the experiment and ends at 1200 UTC on the sixth day. The blue dots and red crosses on the horizontal axis indicate the times of SUMO and radiosonde observations, respectively, used in the assimilation experiments.

lated time series of air temperature, MSLP, wind speed and wind direction at Neumayer III station (see Fig. 1 for the location) for CASE1 and CASE2 (the domain of CASE3 does not cover the station). The distances from Neumayer III station to RV Polarstern range from 305 to 425 km in CASE1 and from 703 to 830 km in CASE2. Generally, the simulations seem to have captured the main variations of air pressure and wind speed. However, the maximum instantaneous difference between the simulated and observed temperature is as large as 10°C. Large errors are found in the simulation of wind direction in CASE1. According to Fig. 4, the simulations with data assimilation (SUMOE and RSE) are nearly identical to the CTRL simulation in all the variables and all cases, indicating that the assimilation of profiles at the site of RV Polarstern had almost no impact on the 1–5-day model experiments for Neumayer station, 300–800 km

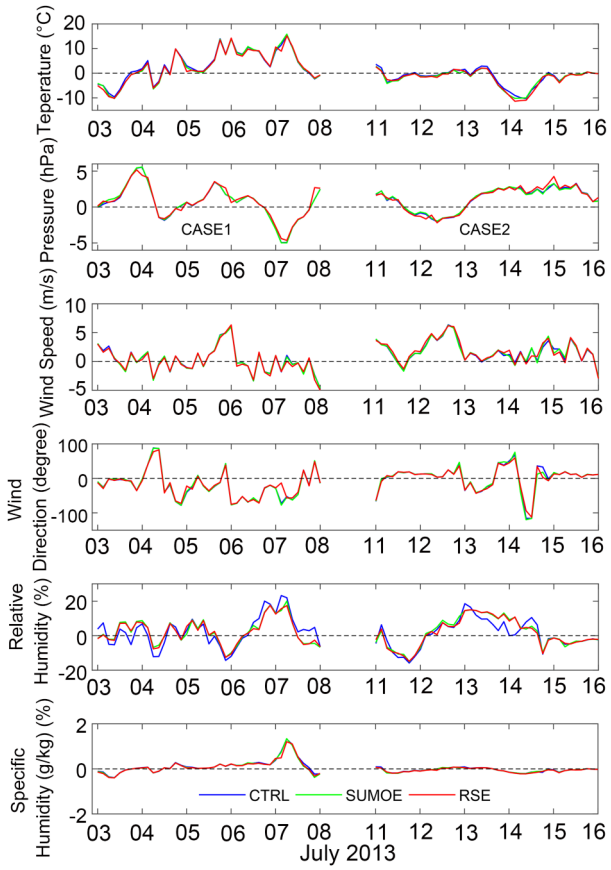

Fig. 4. Time series of the bias (model results minus observations) of surface variables at the location of the Neumayer III station during the CASE1 and CASE2.

apart. This is at least partly due to the fact that during CASE1 and CASE2, only on one day (15 July), the air mass observed by soundings at Polarstern was advected close to Neumayer III station. This has been studied by calculating 5-day forward trajectories and applying the METEX algorithm (Zeng et al., 2010).

To quantify the impact of profile data assimilation, statistics including bias, root-mean-square error (RMSE), and correlation coefficient (R) in the three cases were calculated for the model experiments along the track of RV Polarstern (Table 2). All three simulations in all three cases underestimate the temperature and humidity and overestimate the wind speed (except SUMOE in CASE2). SUMO and RS have a positive impact on the results for air temperature, pressure, wind speed and humidity, seen as better skill scores for SUMOE and RSE than for CTRL (Table 2). RS shows better skill than SUMO in improving the bias in all cases. This is likely due to the much higher observing ceiling of radiosondes (~12 000 m) than SUMO (~1700 m).

3.3. *Impacts on model results on the regional scale*

To find out how the assimilation of sounding data at a single location affects the simulations for the surrounding regions, the results of the CTRL, RSE and SUMOE experiments were compared over a larger area. In lieu of observations, the ECMWF operational analyses were used as a reference. Spatial patterns of the skill scores (bias, RMSE, and R) were calculated for the three experiments in all three cases. First, we selected circles of grid points with distances to the sounding site being multiples of 36 km up to 360 km (i.e., 0 km, 36 km, 72 km, …, 360 km). Then, MSLP, 2-m air temperature and relative humidity values on these points with specific distance were averaged.

We show how the 5-day-averaged values of bias and RMSE for MSLP as well as 2-m air temperature and relative humidity depend on the distance from the observation site (RV Polarstern). From Figs. 5 and 6 we can see that in some cases the bias and RMSE increase and in some cases decrease with distance. For 2-m air temperature the bias and RMSE are almost always smaller in RSE than in SUMOE and CTRL. The same is true for 2-m relative humidity, except for the bias in CASE1. For MSLP, the results vary from case to case, with RSE and SUMOE yielding generally better results than CTRL. As a whole, the results demonstrate that the assimilation of radiosonde and SUMO observations benefit the results of 2-m air temperature and relative humidity, and that the benefit in many cases extends farther than 300 km from the observation site.

4. Discussion and conclusions

We applied the Polar WRF model to test the impact of assimilation of UAV and radiosonde sounding observations

Table 2. Bias (simulations minus observations), RMSE, and correlation coefficient (R) of air temperature (T, in °C), pressure (P, in hPa), wind speed (WS, in m s^{-1}), wind direction (WD, in degrees), relative humidity (RH, in %), and specific humidity (SH, in g kg^{-1}) in the CTRL, SUMOE, and RSE model experiments along the track of RV Polarstern during the three cases.

		T	P	WS	WD	RH	SH
Bias	CTRL	−3.57	−0.50	0.83	−10.00	−8.33	−0.30
	SUMOE	−3.03	−0.53	0.73	−4.00	−7.67	−0.27
	RSE	−2.80	−0.43	0.6	−1.67	−7.33	−0.27
RMSE	CTRL	4.8	1.17	2.4	89.67	11	0.43
	SUMOE	4.43	1.1	2.43	89.33	10.33	0.4
	RSE	4	1.07	2.27	82.67	10	0.37
R	CTRL	0.74	0.99	0.82	0.47	0.32	0.72
	SUMOE	0.73	0.99	0.81	0.47	0.32	0.71
	RSE	0.83	0.99	0.83	0.53	0.4	0.84

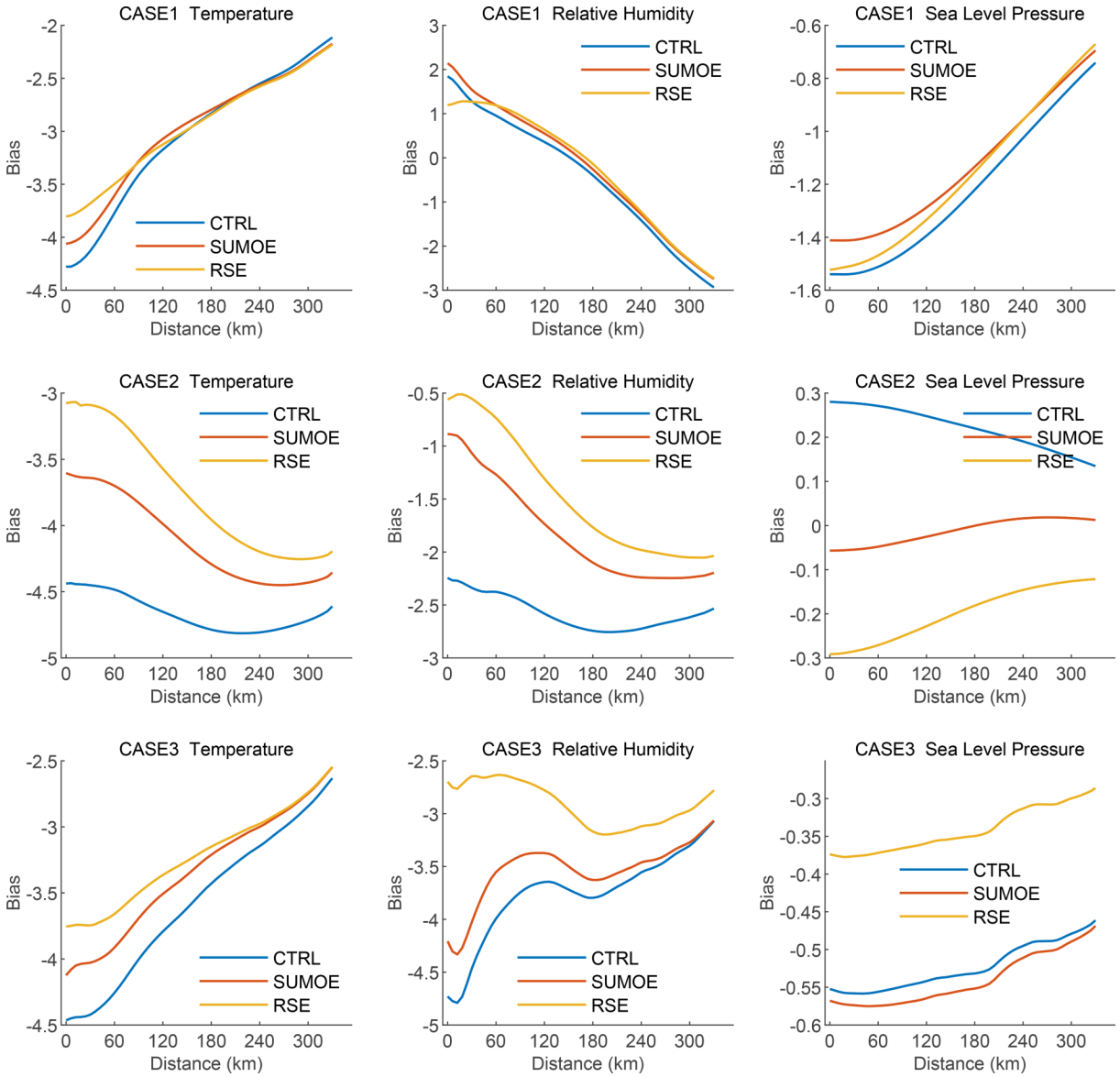

Fig. 5. Dependence of the five-day-averaged bias on the distance from RV Polarstern for 2-m air temperature (°C) and relative humidity (%) and MSLP (hPa).

on model analyses and 5-day-long experiments over the Southern Ocean in winter 2013. The Polar WRF experiments applied the FDDA assimilation method and employed the ECMWF operational analysis as initial and lateral boundary conditions. The assimilation of sounding data from both SUMO and radiosondes improved the analyses of air temperature, wind speed, and air humidity at the observation site for most of the time, but the effects varied between different cases. This may be partly due to the different number of observed profiles in the three cases, and partly due to the different synoptic situations. Considering model results for the sea level pressure and near-surface wind speed, assimilation of radiosonde data was more beneficial than assimilation of UAV data. This is likely due to the higher vertical extent of the radiosonde data. The impact of UAV data assimilation was limited to the layer observed, the lowermost 1–2 km.

All the experiments succeeded in capturing the main features of the evolution of near-surface variables during the 5-day model runs. In the three cases studied, averaged over the five-day periods, the assimilation of radiosonde and UAV data only yielded small benefits for the model results when evaluated against observations at RV Polarstern and the Neumayer III station. We expect that this was partly due to the fact that the comparisons were not made downstream of the sounding sites, as no downstream observations were available (during the cases studied, Neumayer station was not affected by airmass advection from the location of Polarstern). However, the evaluation of the model fields using ECMWF operational analyses as a reference suggested that the benefit from data assimilation was larger. It often reached a distance of 300 km, when results for all directions around the sounding site were averaged.

The positive impact of assimilation of radiosonde data

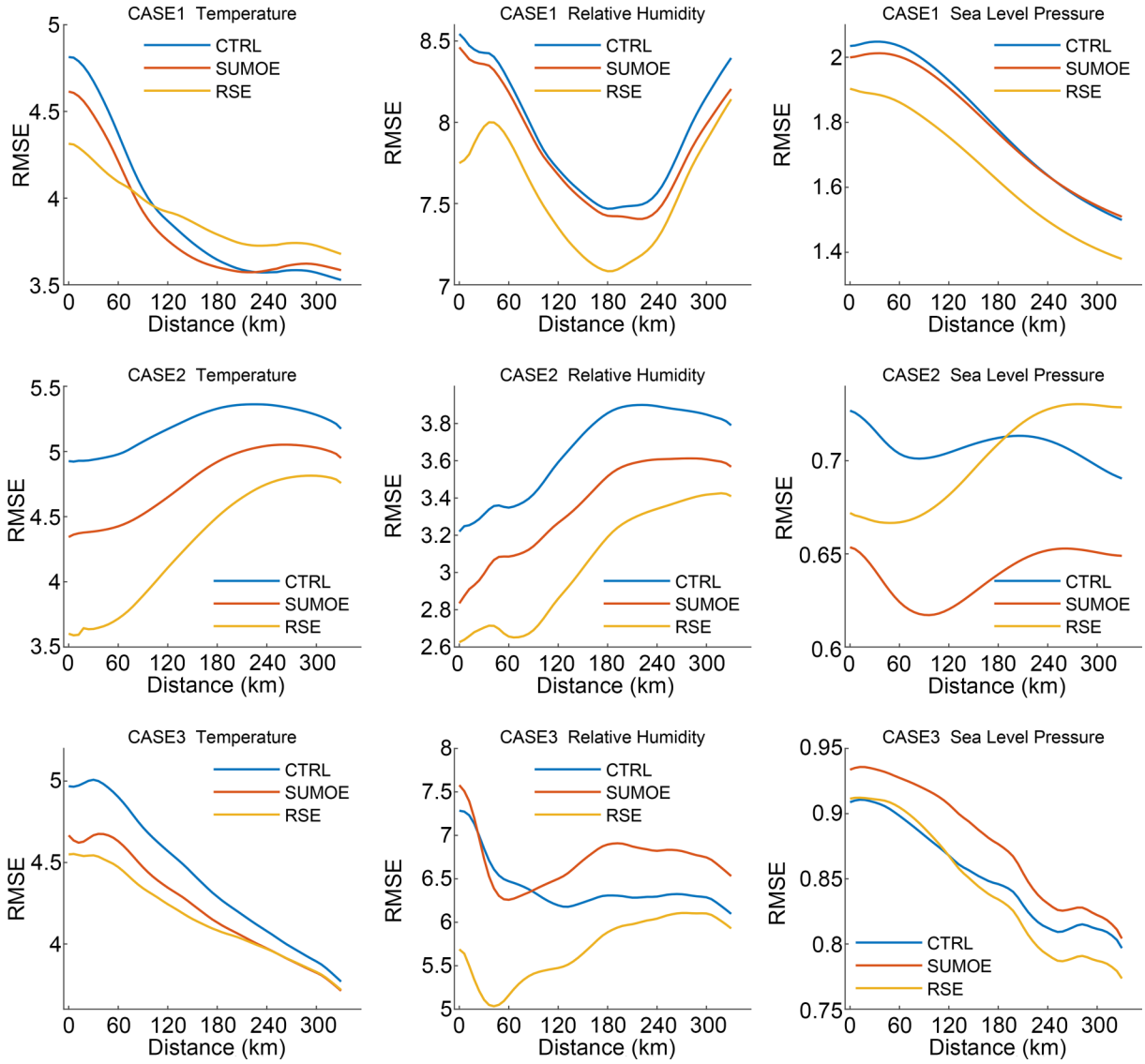

Fig. 6. As in Fig. 5 but for RMSE (same unit as variable).

on analyses and forecasts in the Arctic and Antarctic has been demonstrated by Inoue et al. (2013, 2015), Ono et al. (2016), Sato et al. (2017, 2018), Soldatenko et al. (2018), Lawrence et al. (2019), and Naakka et al. (2019). The finding of Sato et al. (2018) that the benefit of assimilated observations propagated downstream is in line with our results. However, our results are different from previous ones in the following respects. At least four previous studies detected the largest positive impact of radiosonde data assimilation in the upper troposphere and stratosphere (Inoue et al., 2013; Sato et al., 2017, 2018; Lawrence et al., 2019). Upper-tropospheric impacts occurred also in our cases, but in general the data assimilation mostly affected the profiles in the lower troposphere (Fig. 2). Further, in general, our experiments revealed small or moderate impacts of radiosonde and UAV data assimilation. Much larger positive impacts of radiosonde data assimilation have been found in a few previous studies. The model experiments by Inoue et al. (2013) showed that when an exceptionally large amount of radiosonde soundings were available from the Arctic Ocean, the model results were strongly improved: a 5-K cold bias in upper tropospheric temperatures was removed and the tropopause height and subpolar jet stream were affected. Inoue et al. (2015) detected a difference of up to 8 hPa in MSLP between experiments with and without assimilation of campaign-based radiosonde sounding data over the Arctic Ocean, and in an analogous study by Ono et al. (2016) the maximum effect reached 20 hPa. In the cases modeled by Sato et al. (2017), additional Arctic radiosonde soundings had major impacts on the evolution of winter storms over East Asia and North America. The sounding data assimilation improved the analyses particularly in the Arctic upper troposphere, resulting in improved predictions for upper troughs and southward intrusions of high potential vorticity from the Arctic.

Two previous studies have addressed the impact of assimilation of Antarctic radiosonde data on numerical forecasts, both showing large positive effects. In Sato et al. (2018),

assimilation of campaign-based radiosonde sounding data reduced the temperature bias in a layer from 400 to 300 hPa by up to 7 K (in a layer from 1000 to 900 hPa the effect was only of the same magnitude as in our study). The impacts on temperature and geopotential height fields were reflected as improved forecasts for the track of an extratropical cyclone that developed over southeastern Australia and passed near Tasmania in December 2017. The larger impact of sounding data assimilation in the case of Sato et al. (2018) compared to our case is presumably related to the following reasons: a global model was applied and none of the ship radiosonde soundings were sent to GTS. Accordingly, the control experiment was entirely free of the effect of the soundings. In our case, RV Polarstern radiosonde data affected the ECMWF initial and lateral boundary conditions also in the control experiment, presumably reducing the difference between the control experiment and RSE.

In Soldatenko et al. (2018) the focus was on NWP results for Australia, but with a particular interest in the benefit from radiosonde soundings at remote stations. Among the 34 radiosonde stations in the Australian network, the most significant contribution to the reduction of the forecast error indeed originated from the remote Antarctic stations Casey, Davis and Mawson, as well as from Macquarie Island. Soldatenko et al. (2018) further stressed the importance of observations from upstream locations, both from radiosonde stations and ocean buoys.

Common to all studies mentioned above is that they were made applying global models and the forecast lead times were rather long, of the order of 5 to 14 days. Further, the number or frequency of additional observations was larger than in our study cases, when radiosonde soundings were taken only once a day. For example, Inoue et al. (2013) found that increasing the daily soundings from one to two did not yield a positive impact during their study period, and four daily soundings were needed for a positive impact. Another issue common to the above-mentioned studies is that sounding data were assimilated from the entire profile measured. We assimilated data from the lowermost 12-km layer, which covers the entire Antarctic troposphere, but not the stratosphere, which may have contributed to some differences from the results of previous studies.

Although our study demonstrates more benefit from assimilation of radiosonde than SUMO data, the situation may change in the future, when even lower-cost UAVs will potentially be able to measure profiles throughout the troposphere. The advantages of using UAVs instead of radiosondes include at least the following: (1) UAVs can be retrieved and reused, making the operation cost lower than that of radiosondes in the long run; (2) UAVs are better in terms of portability and mobility, allowing changes in the sounding sites to optimally observe different weather systems (although this would not have helped in the present study over the Southern Ocean); (3) both vertical and horizontal profiles can be observed; and (4) the profiles obtained by UAVs are truly vertical, whereas radiosondes can drift tens to hundreds of kilometers during a sounding, thus representing a mixture of horizontal profiles (McGrath et al., 2006). However, we are aware that UAV activities still require manpower, while radiosondes can also be launched automatically. It is, however, foreseen that UAV operations will also be automated in the future. Hence, as all Antarctic observations are expensive and logistically challenging but the technology is continuously evolving, much more work is needed to comprehensively evaluate the costs and benefits that various additional observations could bring to NWP in the Antarctic.

Acknowledgements. This study was supported by the China National Key R&D Program of China (Grant No. 2016YFC140 2705) and the Academy of Finland (contract: 304345). The ECMWF is acknowledged for providing us with the operational analyses. We thank Priit TISLER from Finnish Meteorological Institute for his pivotal contribution to the SUMO observations, the Alfred Wegener Institute for providing us the RV Polarstern radiosonde sounding and AWS data from Polarstern and Neumayer III stations, and the Captain and crew of RV Polarstern for their support during the cruise. This is a contribution to the Year of Polar Prediction (YOPP), a flagship activity of the Polar Prediction Project (PPP), initiated by the World Weather Research Programme (WWRP) of the World Meteorological Organisation (WMO). We acknowledge the WMO WWRP for its role in coordinating this international research activity.

REFERENCES

Agustí-Panareda, A., A. Beljaars, C. Cardinali, I. Genkova, and C. Thorncroft, 2010: Impacts of assimilating AMMA soundings on ECMWF analyses and forecasts. *Wea. Forecasting*, **25**(4), 1142–1160, https://doi.org/10.1175/2010WAF2222370.1.

Ágústsson, H., H. Ólafsson, M. O. Jonassen, and Ó. Rögnvaldsson, 2014: The impact of assimilating data from a remotely piloted aircraft on simulations of weak-wind orographic flow. *Tellus A: Dynamic Meteorology and Oceanography*, **66**(1), 25421, https://doi.org/10.3402/tellusa.v66.25421.

Atlaskin, E., and T. Vihma, 2012: Evaluation of NWP results for wintertime nocturnal boundary-layer temperatures over Europe and Finland. *Quart. J. Roy. Meteorol. Soc.*, **138**(667), 1440–1451, https://doi.org/10.1002/qj.1885.

Båserud, L., J. Reuder, M. O. Jonassen, S. T. Kral, M. B. Paskyabi, and M. Lothon, 2016: Proof of concept for turbulence measurements with the RPAS SUMO during the BLLAST campaign. *Atmospheric Measurement Techniques*, **9**(10), 4901–4913, https://doi.org/10.5194/amt-9-4901-2016.

Bouchard, A., F. Rabier, V. Guidard, and F. Karbou, 2010:

Enhancements of satellite data assimilation over Antarctica. *Mon. Wea. Rev.*, **138**(6), 2149–2173, https://doi.org/10.1175/2009MWR3071.1.

Boylan, P., J. H. Wang, S. A. Cohn, E. Fetzer, E. S. Maddy, and S. Wong, 2015: Validation of AIRS version 6 temperature profiles and surface-based inversions over Antarctica using Concordiasi dropsonde data. *J. Geophys. Res.*, **120**(3), 992–1007, https://doi.org/10.1002/2014JD022551.

Bromwich, D. H., A. J. Monaghan, K. W. Manning, and J. G. Powers, 2005: Real-time forecasting for the Antarctic: An evaluation of the Antarctic Mesoscale Prediction System (AMPS). *Mon. Wea. Rev.*, **133**(3), 579–603, https://doi.org/10.1175/MWR-2881.1.

Bromwich, D. H., F. O. Otieno, K. M. Hines, K. W. Manning, and E. Shilo, 2013: Comprehensive evaluation of polar weather research and forecasting model performance in the Antarctic *J.GeophysRes.*,**118**(2),274–292,https://doi.org/10.1029/2012JD018139.

Bromwich, D. H., A. B. Wilson, L. S. Bai, G. W. K. Moore, and P. Bauer, 2016: A comparison of the regional Arctic System Reanalysis and the global ERA-Interim Reanalysis for the Arctic. *Quart. J. Roy. Meteorol. Soc.*, **142**, 644–658, https://doi.org/10.1002/qj.2527.

Bumbaco, K. A., G. J. Hakim, G. S. Mauger, N. Hryniw, and E. J. Steig, 2014: Evaluating the Antarctic observational network with the Antarctic Mesoscale Prediction System (AMPS). *Mon. Wea. Rev.*, **142**(10), 3847–3859, https://doi.org/10.1175/MWR-D-13-00401.1.

Cassano, J. J., 2014: Observations of atmospheric boundary layer temperature profiles with a small unmanned aerial vehicle. *Antarctic Science*, **26**(2), 205–213, https://doi.org/10.1017/S0954102013000539.

Cassano, J. J., M. W. Seefeldt, S. Palo, S. L. Knuth, A. C. Bradley, P. D. Herrman, P. A. Kernebone, and N. J. Logan, 2016: Observations of the atmosphere and surface state over Terra Nova Bay, Antarctica, using unmanned aerial systems. *Earth System Science Data*, **8**(1), 115–126, https://doi.org/10.5194/essd-8-115-2016.

Caumont, O., and Coauthors, 2016: Assimilation of humidity and temperature observations retrieved from ground-based microwave radiometers into a convective-scale NWP model. *Quart. J. Roy. Meteorol. Soc.*, **142**(700), 2692–2704, https://doi.org/10.1002/qj.2860.

Dee, D. P., and Coauthors, 2011: The ERA-Interim reanalysis: Configuration and performance of the data assimilation system. *Quart. J. Roy. Meteorol. Soc.*, **137**(656), 553–597, https://doi.org/10.1002/qj.828.

Derber, J. C., and W. S. Wu, 1998: The use of TOVS cloud-cleared radiances in the NCEP SSI analysis system. *Mon. Wea. Rev.*, **126**, 2287–2299, https://doi.org/10.1175/1520-0493(1998)126<2287:TUOTCC>2.0.CO;2.

Driemel, A., B. Loose, H. Grobe, R. Sieger, and G. König-Langlo, 2016: 30 years of upper air soundings on board of R/V *POLARSTERN*. *Earth System Science Data*, **8**(1), 213–220, https://doi.org/10.5194/essd-8-213-2016.

Federico, S., 2013: Implementation of a 3D-Var system for atmospheric profiling data assimilation into the RAMS model: Initial results. *Atmospheric Measurement Techniques*, **6**(12), 3563–3576, https://doi.org/10.5194/amt-6-3563-2013.

Grell, G. A., and D. Dévényi, 2002: A generalized approach to parameterizing convection combining ensemble and data assimilation techniques. *Geophys. Res. Lett.*, **29**(14), 1693, https://doi.org/10.1029/2002GL015311.

Guedj, S., F. Karbou, F. Rabier, and A. Bouchard, 2010: Toward a better modeling of surface emissivity to improve AMSU data assimilation over Antarctica. *IEEE Trans. Geosci. Remote Sens.*, **48**(4), 1976–1985, https://doi.org/10.1109/TGRS.2009.2036254.

Hines, K. M., and D. H. Bromwich, 2008: Development and testing of Polar Weather Research and Forecasting (WRF) model. *Part I: Greenland ice sheet meteorology. Mon. Wea. Rev.*, **136**(6), 1971–1989, https://doi.org/10.1175/2007MWR2112.1.

Hines, K. M., and D. H. Bromwich, 2017: Simulation of late summer arctic clouds during ASCOS with polar WRF. *Mon. Wea. Rev.*, **145**(2), 521–541, https://doi.org/10.1175/MWR-D-16-0079.1.

Iacono, M. J., J. S. Delamere, E. J. Mlawer, M. W. Shephard, S. A. Clough, and W. D. Collins, 2008: Radiative forcing by long-lived greenhouse gases: Calculations with the AER radiative transfer models. *J. Geophys. Res.*, **113**(D13), D13103, https://doi.org/10.1029/2008JD009944.

Inoue, J., T. Enomoto, and M. E. Hori, 2013: The impact of radiosonde data over the ice-free Arctic Ocean on the atmospheric circulation in the Northern Hemisphere. *Geophys. Res. Lett.*, **40**(5), 864–869, https://doi.org/10.1002/grl.50207.

Inoue, J., A. Yamazaki, J. Ono, K. Dethloff, M. Maturilli, R. Neuber, P. Edwards, and H. Yamaguchi, 2015: Additional Arctic observations improve weather and sea-ice forecasts for the Northern Sea Route. *Scientific Reports*, **5**, 16868, https://doi.org/10.1038/srep16868.

Janjić, Z. I., 2001: Nonsingular implementation of the Mellor-Yamada level 2.5 scheme in the NCEP meso model. NCEP Technical Report 437, 61 pp.

Jonassen, M., and J. Reuder, 2008: Determination of temperature and humidity profiles in the atmospheric boundary layer by fast ascending UAVs. Geophysical Research Abstracts.

Jonassen, M. O., H. Ólafsson, H. Ágústsson, Ó. Rögnvaldsson, and J. Reuder, 2012: Improving high-resolution numerical weather simulations by assimilating data from an unmanned aerial system. *Mon. Wea. Rev.*, **140**(11), 3734–3756, https://doi.org/10.1175/MWR-D-11-00344.1.

Jonassen, M. O., P. Tisler, B. Altstädter, A. Scholtz, T. Vihma, A. Lampert, G. König-Langlo, and C. Lüpkes, 2015: Application of remotely piloted aircraft systems in observing the atmospheric boundary layer over Antarctic sea ice in winter. *Polar Research*, **34**, 25651, https://doi.org/10.3402/polar.v34.25651.

Jones, J. M., and Coauthors, 2016: Assessing recent trends in high-latitude Southern Hemisphere surface climate. *Nat. Clim. Change*, **6**(10), 917–926, https://doi.org/10.1038/nclimate3103.

Karbou, F., 2014: The assimilation of observations from the advanced microwave sounding unit over sea ice in the French global numerical weather prediction system. *Mon. Wea. Rev.*, **142**(1), 125–140, https://doi.org/10.1175/MWR-D-13-00025.1.

Knupp, K. R., T. Coleman, D. Phillips, R. Ware, D. Cimini, F. Vandenberghe, J. Vivekanandan, and E. Westwater, 2009: Ground-based passive microwave profiling during dynamic weather conditions. *J. Atmos. Oceanic Technol.*, **26**(6), 1057–1073, https://doi.org/10.1175/2008JTECHA1150.1.

Knuth, S. L, J. J. Cassano, J. A. Maslanik, P. D. Herrmann, P. A.

Kernebone, R. I. Crocker, and N. J. Logan, 2013: Unmanned aircraft system measurements of the atmospheric boundary layer over Terra Nova Bay, Antarctica. *Earth System Science Data*, **5**(1), 57–69, https://doi.org/10.5194/essd-5-57-2013.

König-Langlo, G., 2013a: Meteorological observations during POLARSTERN cruise ANT-XXIX/6(AWECS). Alfred Wegener Institute, Helmholtz Centre for Polar and Marine Research, Bremerhaven, PANGAEA, https://doi.org/10.1594/PANGAEA.819610.

König-Langlo, G., 2013b: Upper air soundings during POLARSTERN cruise ANT-XXIX/6(AWECS) to the Antarctic in 2013. Alfred Wegener Institute, Helmholtz Centre for Polar and Marine Research, Bremerhaven, PANGAEA, https://doi.org/10.1594/PANGAEA.842810.

Kral, S. T., and Coauthors, 2018: Innovative strategies for observations in the arctic atmospheric boundary layer (ISOBAR)–The Hailuoto 2017 campaign. *Atmosphere*, **9**, 268, https://doi.org/10.3390/atmos9070268.

Lawrence, H., N. Bormann, I. Sandu, J. Day, J. Farnan, and P. Bauer., 2019: Use and impact of arctic observations in the ECMWF numerical weather prediction system. *Quart. J. Roy. Meteorol. Society*, **145**(725), 3432–3454, https://doi.org/10.1002/qj.3628.

Luers, J. K. and Eskridge, R. E., 1998: Use of radiosonde temperature data in climate studies. *J. Climate*, **11**(5), 1002–1019, https://doi.org/10.1175/1520-0442(1998)011<1002:UORTDI>2.0.CO;2.

Mayer, S., 2011: Application and improvement of the Unmanned Aerial System SUMO for atmospheric boundary layer studies. PhD dissertation, University of Bergen, 93 pp.

McGrath, R., T. Semmler, C. Sweeney, and S. Y. Wang, 2006: Impact of balloon drift errors in radiosonde data on climate statistics.*J.Climate*,**19**(14),3430–3442,https://doi.org/10.1175/JCLI3804.1.

Miloshevich, L. M., A. Paukkunen, H. Vömel, and S. J. Oltmans, 2004: Development and validation of a time-lag correction for Vaisala radiosonde humidity measurements. *J. Atmos. Oceanic Technol.*, **21**(9), 1305–1327, https://doi.org/10.1175/1520-0426(2004)021<1305:DAVOAT>2.0.CO;2.

Murphy, D. J., S. P. Alexander, A. R. Klekociuk, P. T. Love, and R. A. Vincent, 2014: Radiosonde observations of gravity waves in the lower stratosphere over Davis, Antarctica. *J. Geophys. Res.*, **119**(21), 11973–11996, https://doi.org/10.1002/2014JD022448.

Naakka, T., T. Nygård, M. Tjernström, T. Vihma, R. Pirazzini, and I. M. Brooks, 2019: The impact of radiosounding observations on numerical weather prediction analyses in the Arctic. *Geophys. Res. Lett.*, **46**(14), 8527–8535, https://doi.org/10.1029/2019GL083332.

National Weather Service, 2019: Frequently asked question about radiosonde data quality. [Available online from https://www.weather.gov/upperair/FAQ-QC]

Ono, J., J. Inoue, A. Yamazaki, K. Dethloff, and H. Yamaguchi, 2016: The impact of radiosonde data on forecasting sea-ice distribution along the Northern Sea Route during an extremely developed cyclone. *Journal of Advances in Modeling Earth Systems*, **8**(1), 292–303, https://doi.org/10.1002/2015MS000552.

Passner, J. E., S. Kirby, and T. Jameson, 2012: Using real-time weather data from an unmanned aircraft system to support the advanced research version of the weather research and forecast model. No. ARL-TR-5950, Army Research Laboratory, USA, 70 pp.

Powers, J. G., K. W. Manning, D. H. Bromwich, J. J. Cassano, and A. M. Cayette, 2012: A decade of Antarctic science support through AMPS. *Bull. Amer. Meteor. Soc.*, **93**(11), 1699–1712, https://doi.org/10.1175/BAMS-D-11-00186.1.

Reuder, J., P. Brisset, M. Jonassen, M. Müller, and S. Mayer, 2009: The small unmanned meteorological observer SUMO: A new tool for atmospheric boundary layer research. *Meteorologische Zeitschrift*, **18**(2), 141–147, https://doi.org/10.1127/0941-2948/2009/0363.

Rintoul, S. R., M. Sparrow, M. Meredith, V. Wadley, K. Speer, E. Hofmann, and K. Alverson, 2012: *The Southern Ocean Observing System: Initial Science and Implementation Strategy*. Scientific Committee on Antarctic Research, 82 pp.

Sato, K., J. Inoue, A. Yamazaki, J.-H. Kim, M. Maturilli, K. Dethloff, S. R. Hudson, and M. A. Granskog, 2017: Improved forecasts of winter weather extremes over midlatitudes with extra Arctic observations. *J. Geophys. Res.*, **122**(2), 775–787, https://doi.org/10.1002/2016JC012197.

Sato, K., J. Inoue, S. P. Alexander, G. McFarquhar, and A. Yamazaki, 2018: Improved reanalysis and prediction of atmospheric fields over the Southern Ocean using campaign-based radiosonde observations. *Geophys. Res. Lett.*, **45**(20), 11406–11413, https://doi.org/10.1029/2018GL079037.

Singh, R., C. M. Kishtawal, S. P. Ojha, and P. K. Pal, 2012: Impact of assimilation of Atmospheric InfraRed Sounder (AIRS) radiances and retrievals in the WRF 3D-Var assimilation system. *J. Geophys. Res.*, **117**(D11), D11107, https://doi.org/10.1029/2011JD017367.

Soldatenko, S., C. Tingwell, P. Steinle, and B. A. Kelly-Gerreyn, 2018: Assessing the impact of surface and upper-air observations on the forecast skill of the ACCESS numerical weather prediction model over Australia. *Atmosphere*, **9**(1), 23, https://doi.org/10.3390/atmos9010023.

Turner, J., and S. Pendlebury, 2004: *The International Antarctic Weather Forecasting Handbook*. British Antarctic Survey, Cambridge, United Kingdom, 663 pp.

Wille, J. D., D. H. Bromwich, J. J. Cassano, M. A. Nigro, M. E. Mateling, and M. A. Lazzara, 2017: Evaluation of the AMPS boundary layer simulations on the ross ice shelf, Antarctica, with unmanned aircraft observations. *J. Appl. Meteorol. Climatol.*, **56**(8), 2239–2258, https://doi.org/10.1175/JAMC-D-16-0339.1.

Yamazaki, A., J. Inoue, K. Dethloff, M. Maturilli, and G. König-Langlo, 2015: Impact of radiosonde observations on forecasting summertime Arctic cyclone formation. *J. Geophys. Res.*, **120**(8), 3249–3273, https://doi.org/10.1002/2014JD022925.

Zeng, J., T. Matsunaga, and H. Mukai, 2010: METEX–A flexible tool for air trajectory calculation. *Environmental Modelling & Software*, **25**(4), 607–608, https://doi.org/10.1016/j.envsoft.2008.10.015.